

# Molecular magnetic resonance probe targeting VEGF165: preparation and *in vitro* and *in vivo* evaluation

Xiao-Guang You<sup>a</sup>, Rong Tu<sup>a\*</sup>, Ming-Li Peng<sup>b</sup>, Yu-Jie Bai<sup>a\*</sup>, Mingqian Tan<sup>c</sup>, Han-Jian Li<sup>a</sup>, Jing Guan<sup>d</sup> and Li-Jun Wen<sup>e</sup>

A new method for imaging the tumor human vascular endothelial growth factor 165 (VEGF 165) is presented. A magnetic resonance imaging (MRI) probe was prepared by crosslinking ultrasmall superparamagnetic iron oxide (USPIO) nanoparticles to the aptamer for tumor vascular endothelial growth factor 165 (VEGF165-aptamer). The molecular probe was evaluated for its *in vitro* and *in vivo* activities toward VEGF165. Enzyme-linked immunosorbent assay showed that the VEGF165-aptamer-USPIO nanoparticles conjugate specifically binds to VEGF165 *in vitro*. A cell proliferation test showed that VEGF165-aptamer-USPIO seems to block the proliferation of human umbilical vein endothelial cells induced by free VEGF165, suggesting that VEGF165 is an effective target of this molecular probe. In xenograft mice carrying liver cancer that expresses VEGF165, T<sub>2</sub>-weighted imaging of the tumor displayed marked negative enhancement 3 h after the intravenous administration of VEGF165-aptamer-USPIO. The enhancement disappeared 6 h after administration of the probe. These results suggest the targeted imaging effect of VEGF165-aptamer-USPIO probe *in vivo* for VEGF165-expressing tumors. This is the first report of a targeted MRI molecular probe based on USPIO and VEGF165-aptamer. Copyright © 2014 John Wiley & Sons, Ltd.

**Keywords:** VEGF165; aptamer; (USPIO); targeted molecular probe; MRI; liver cancer

## 1. INTRODUCTION

Angiogenesis plays an important regulatory role in tumor growth, progression and migration. Evaluation of angiogenesis by molecular imaging contributes to early diagnosis, more effective targeted treatment and better prognosis for cancer (1). Tumor angiogenesis is a complex, multistep process that requires the interaction of multiple factors, which need to be coordinated in specific space and time domains. Among the many tumor angiogenesis regulatory factors, vascular endothelial growth factor (VEGF) plays an important role and is present in a large variety of malignant tumors (2). VEGF functions by binding to its receptor in the plasma membrane of vascular endothelial cells, and then activating the protein kinase C signal transduction pathway. Because of its role in maintaining tumor angiogenesis and proliferation, VEGF is a useful biomarker for tumor metabolism and metastasis (3).

Several methods for imaging VEGF have been reported, such as the use of radioisotope-labeled VEGF monoclonal antibodies for PET imaging. As early as 2002, <sup>124</sup>I-HuMV833 (humanized anti-VEGF-A mouse monoclonal antibody) entered a phase I clinical trial for imaging-based evaluation of cancer treatment outcomes (4). More recently, <sup>89</sup>Zr-bevacizumab (VEGF recombinant humanized monoclonal antibody) was shown to be a sensitive agent for monitoring tumor treatment efficacy (5); however, its application has been limited by its potent immunogenicity, and methods to accurately dose this contrasting agent in various tumors and patients remain to be established. For targeted ultrasound imaging, the scVEGF-bearing microbubble contrast agent showed significant signal enhancement in the imaging of

tumors; however, this technique is limited by the relatively poor resolution and tissue penetration of ultrasound imaging (6).

Because magnetic resonance imaging (MRI) displays high soft tissue resolution and spatial anatomical resolution, molecular probes targeting VEGF or VEGF receptor have been developed for targeted MRI. For example, a gadolinium-conjugated anti-VEGF antibody showed significantly increased and prolonged signal enhancement in the imaging of tumors, compared with non-targeted imaging (7). However, the large molecular weight and *in vivo* immunogenicity issues of antibodies have caused

\* Correspondence to: Rong Tu and Yu-jie Bai, Hainan Medical College, Haikou City, Hainan Province 570102, China. E-mail: turong37472@126.com; yujiebai2008@gmail.com

a X.-G. You, R. Tu, Y.-J. Bai, H.-J. Li  
Department of Radiology and Cancer Institute, Hainan Medical College Hospital, Haikou City, Hainan Province 570102, China

b M.-L. Peng  
Northwest University, Xi'an City, Shanxi Province 710068, China

c M. Tan  
Laboratory of Biomedical Materials Engineering, Dalian Institute of Chemical Physics, Chinese Academy of Sciences, Dalian 116023, China

d J. Guan  
Department of Radiology, Zhunyi Medical College Hospital, Zhunyi City, Guizhou Province 564400, China

e L.-J. Wen  
School of Pharmacy, Hainan Medical College, Haikou City, Hainan Province 571101, China

researchers to turn to aptamers as an alternative targeting agent for imaging. Aptamers have several advantages over antibodies. They are not limited by immune recognition or immunogenicity; they can be artificially synthesized and modified *in vitro*; their denaturation is reversible; and they can be transported and stored on a long-term basis at room temperature (8–10). A good example is the aptamer for VEGF165 (VEGF165-aptamer), which is a single-chain oligonucleotide fragment that binds specifically to VEGF165 (11).

VEGF165 is the predominant and most active VEGF subtype *in vivo*, and it is the most frequently used subtype in medical practice and research. It promotes the proliferation of vascular endothelial cells, increases blood vessel permeability and induces tumor angiogenesis. VEGF165 expression is very low under physiological conditions, and a reasonable level of expression is only found in embryonic tissues and proliferative endothelium. For these reasons, VEGF165 is an important target molecule for tumor imaging and treatment, and it is an ideal target for the construction of a molecular imaging probe.

In this report, we describe the preparation of tumor targeted VEGF165-aptamer-USPIO probe by chemically crosslinking ultrasmall superparamagnetic iron oxide (USPIO) nanoparticles and the aptamer specific for VEGF165. We examined the negative MR targeted VEGF165-aptamer-USPIO probe, and observed its *in vitro* binding activity to VEGF165 and a targeted MR imaging effect in tumor xenograft mice. As far as we know, this is the first report of an aptamer-based MRI molecular probe targeting VEGF165.

## 2. RESULTS AND DISCUSSION

The preparation and testing of molecular probes for MRI have been well studied (12–14). An ideal MRI molecular probe must have both high selectivity and affinity for the target biomolecule, and it should be able to reflect the amount of this biomolecule *in vivo*. The probe should display no differential binding affinity for the same target molecule as a function of its location in the plasma membrane or the cytoplasm. High permeability is important so that it quickly reaches the target. The probe should not induce a significant immune reaction or other adverse reactions. It must be fairly stable *in vivo*, and at the same time have a targeting moiety that allows selective binding with the target biomolecule without generating a high background in circulation (15–18).

VEGF165-aptamer is a 27-base small molecule oligonucleotide, in which all pyrimidines are fluorinated at the 2' position of the ribose ring and all purines are methylated at the 2' position. The aptamer is not degraded by RNAase in its natural environment. It recognizes the target molecular through its heparin binding domain, and it binds to the target molecule with high affinity (11). VEGF165 is an ideal target for molecular imaging owing to its potent angiogenic effect and differential expression in both normal and proliferative tumor tissues. Therefore, we prepared an aptamer-based MRI contrast agent targeting VEGF165, and tested its *in vitro* and *in vivo* activities.

The targeted magnetic contrast agent, USPIO-VEGF165-aptamer, was prepared by chemically crosslinking the negative magnetic resonance contrast USPIO to VEGF165-aptamer. The carboxyl groups on the surface of glucose-coated USPIO were activated by *N*-(3-dimethylaminopropyl)-*N*-ethylcarbodiimide (EDC) and *N*-hydroxysuccinimide (NHS) to react with the amino groups of

VEGF165-aptamer to form stable linkages (Fig. 1) (19), with an estimated yield was of about 90%. The diameter of the USPIO nanoparticles was estimated to be about 20 nm with transmission electron microscopy (Fig. 2). To confirm that the VEGF-aptamer-USPIO probe was in fact superparamagnetic, the magnetic behavior was tested and no hysteresis loop was found, suggesting that the VEGF-aptamer-USPIO probe is superparamagnetic with a magnetic saturation moment of 35 emu/g (Fig. 3). The crosslinking of USPIO nanoparticles to the aptamer was analyzed by gel electrophoresis experiment (Fig. 4). The negatively charged

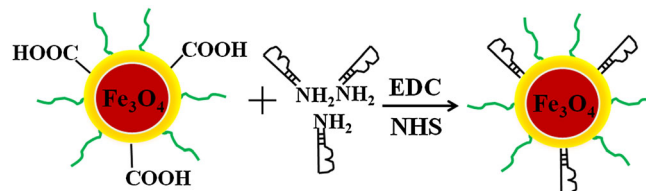


**Figure 1.** The preparation of VEGF165-aptamer-USPIO probe by chemically crosslinking ultrasmall superparamagnetic iron oxide (USPIO) nanoparticles and aptamer for tumor vascular endothelial growth factor 165 (VEGF165-aptamer). The carboxyl groups of glucose-coated USPIO nanoparticles are activated by *N*-(3-dimethylaminopropyl)-*N*-ethylcarbodiimide (EDC) and *N*-hydroxysuccinimide (NHS), and then reacted with the amino groups of VEGF165-aptamer.

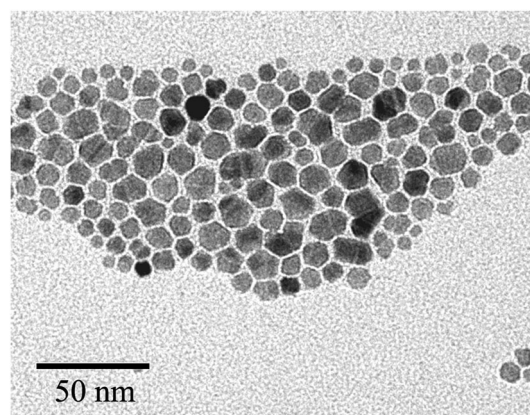


**Figure 2.** Transmission electron microscopy of VEGF165-aptamer-USPIO nanoparticles. Diameters are estimated to be about 20 nm.

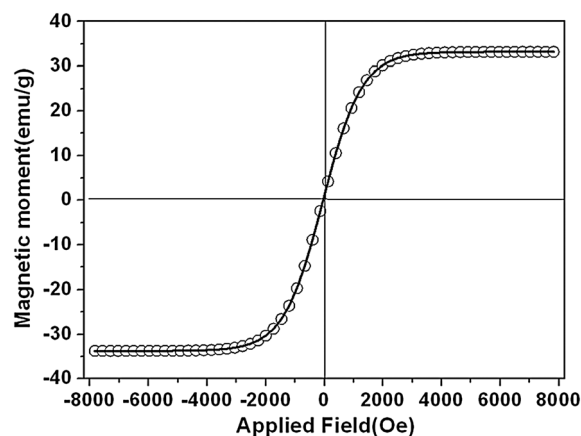


**Figure 3.** Hysteresis loop of the VEGF165-aptamer-USPIO probe measured at 300 K.

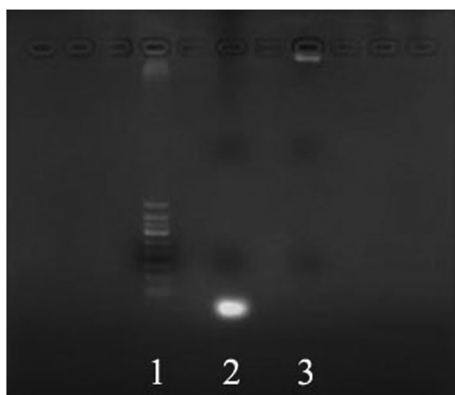


**Figure 4.** Gel electrophoresis of VEGF165-aptamer-USPIO probe. VEGF165-aptamer was methylated and fluorinated before being subjected to 1.8% agarose electrophoresis. The band of VEGF165-aptamer (2) is below the 50 bp marker band (1). The band of VEGF165-aptamer-USPIO nanoparticles (3) is immediately below the gate of the electrophoresis channel, consistent with the hindering effect of USPIO nanoparticles on mobility.

VEGF165-aptamer (band 2 in Fig. 4) can move to the anode. After modification with VEGF165-aptamer, the migration of VEGF165-aptamer-USPIO probe was hindered by the natural charged USPIO nanoparticles (band 3 in Fig. 4), revealing that the aptamer was successfully conjugated on the surface of the USPIO nanoparticles.

An important parameter for the evaluation of a targeted molecular contrast agent is its selectivity for the target molecule.

Enzyme linked immunosorbent assay (ELISA) showed that VEGF165-aptamer-USPIO probe binds specifically to VEGF165 but not to VEGF121 *in vitro* (Table 1). This specific binding activity and the irreversible stable chemical link between USPIO and VEGF165-aptamer were the foundation for the subsequent *in vitro* and *in vivo* targeting VEGF165 studies. Furthermore, the proliferation of human umbilical vein endothelial cells (HUVEC) was evaluated by using the cell counting kit-8 (CCK-8) at the presence of the VEGF165-aptamer-USPIO probe. Unlike tumor cells that secrete VEGF165 themselves and thus interfere with the result in this study, HUVEC were chosen for this study because they do not secrete VEGF165 and their growth is very sensitive to a change in VEGF165 in the surrounding environment. CCK-8 allows sensitive colorimetric assays for the determination of cell viability in cell proliferation (20). CCK-8 is more stable than other tetrazolium salts such as MTT (Methylthiazolyldiphenyl-tetrazolium bromide). The CCK-8 assay of HUVEC proliferation showed that VEGF165-aptamer-USPIO probe can block HUVEC proliferation induced by a fixed amount of externally added VEGF165 (Table 2). This indicated the presence of the VEGF165-aptamer on the USPIO nanoparticles' surface, which can interact with VEGF165-induced HUVEC cells and affect their proliferation. All these results suggested that the VEGF165-aptamer-USPIO might have potential as a probe for tumor targeted MR imaging.

To verify the ability of VEGF165-aptamer-USPIO probe to target VEGF165 *in vivo*, we examined  $T_2$ -weighted imaging ( $T_2WI$ ) contrast enhancement in a xenograft mice model that carries subaxillary liver cancer. Table 3 shows the signal-to-noise ratio (SNR) of the mouse xenografts before and after the admin-

**Table 1.** ELISA of the *in vitro* binding of VEGF165-aptamer-USPIO and VEGF165

Group no.	Assay components	$A_{450} (\bar{x} \pm s)$	Statistical Analysis	
			groups	$p$
1	USPIO + VEGF165	$0.81 \pm 0.01$	1 vs 2	< 0.001
2	VEGF165-Aptamer-USPIO + VEGF165	$2.52 \pm 0.06$	2 vs 3	< 0.001
3	VEGF165-Aptamer-USPIO + VEGF121	$0.81 \pm 0.01$	1 vs 3	0.729

Data were analyzed using the  $t$  test (for instance least significant difference, LSD,  $t$ ),  $F = 3455$ , statistical values are partially given for intergroup comparisons. The difference is considered statistically significant when  $p < 0.05$ .

USPIO, ultrasmall superparamagnetic iron oxide; VEGF165-aptamer, aptamer for tumor vascular endothelial growth factor 165.

**Table 2.** The effect of VEGF165-aptamer-USPIO probe on VEGF165-induced cell proliferation

Group no.	VEGF165-aptamer-USPIO (mg/ml)	VEGF165 (ng/ml)	$OD_{450} (\bar{x} \pm s)$	Statistical analysis	
				Groups	$p$ -Value
1	0	0	$0.980 \pm 0.002$	1 vs 2	<0.001
2	0.5	8.89	$1.218 \pm 0.003$	2 vs 3	<0.001
3	0.25	8.89	$1.806 \pm 0.003$	3 vs 4	<0.001
4	0.125	8.89	$1.904 \pm 0.002$	4 vs 5	<0.001
5	0	8.89	$2.212 \pm 0.007$	5 vs 1	<0.001

Group 1 is the negative control, groups 2–4 are the experimental groups, adding different concentration VEGF165-aptamer-USPIO to the HUVEC cells in the presence of free VEGF165. Group 5 is the positive control, adding free VEGF165 only. Data is analyzed using the  $t$ -test (for instance LSD- $t$ ),  $F = 17180$ , partially given is the statistical value from intergroup comparisons. \* The difference is considered statistically significant when  $p < 0.05$ . Cell concentration is 1000 per well. Volume of the cultured media is 0.225 ml.

**Table 3.** Tumor  $T_2$  signal-to-noise ratio before (pre-injection) and at various time points after the administration of VEGF165-aptamer-USPIO or USPIO to xenograft-bearing mice ( $\bar{x} \pm s$ ,  $n = 15$ ) from tail vein

Group	Signal-to-noise ratio				F	$p^*$
	Pre-injection	3 h	6 h	24 h		
A ( $n = 7$ )	$7.89 \pm 1.52$	$3.27 \pm 2.77$	$7.58 \pm 2.64$	$7.54 \pm 1.65$	5.54	0.03
B ( $n = 8$ )	$8.93 \pm 1.22$	$9.32 \pm 2.08$	$8.59 \pm 1.43$	$8.17 \pm 2.59$	1.43	0.27
F	1.17	35.21	1.5	0.3		
$p^\#$	0.29	0	0.243	0.593		

Mice of group A and B were administered VEGF165-aptamer-USPIO and USPIO, respectively, from tail vein. <sup>a</sup> In group A, the signal-to-noise ratio of tumor 3 h post-injection was statistically different from that pre-injection, and 6 and 24 h after the contrast administration ( $p < 0.05$ ). The SNR of tumors in group B (control) did not show significant difference ( $p = 0.27$ ).

istration of VEGF165-aptamer-USPIO and USPIO nanoparticles. As shown in Fig. 5, 3 h after the administration of VEGF165-aptamer-USPIO probe through the mice tail vein, the SNR of the tumor was markedly lower than that of the pre-injection of the agent ( $p < 0.05$ ; Fig. 6). This negative enhancement phenomenon completely disappeared 6 h after the injection of the probe ( $p < 0.05$ ; Fig. 6). In a sharp contrast, the SNR of the mice xenografts remained essentially unchanged before and after the same amount of USPIO administration by the same route (Fig. 6). These results clearly suggest the VEGF165-aptamer-USPIO probe can accumulate in tumor and generate the magnetic signal enhancement effect.

The maximum negative enhancement effect occurred at 3 h after contrast administration, which has never been reported in previous targeted USPIO-related studies. Hsieh *et al.* reported a VEGF antibody-conjugated USPIO, which was given to the mice bearing CT26 colon cancer xenograft through the tail vein. Tumor  $T_2$ WI signal started to decrease 1 h after the contrast administration; the lowest  $T_2$ WI signal and the maximum enhancement effect occurred 1–2 days after contrast administration; and the enhancement effect gradually disappeared over the next 9 days (21). Leung *et al.* reported a USPIO conjugated to the ovarian cancer OCMab183B2 antibody (22). The lowest  $T_2$ WI signal and maximum negative enhancement occurred 24 h after the contrast was given to mice bearing a subcutaneous SKOV ovarian cancer xenograft, and the enhancement effect gradually disappeared in the next 24 h. The maximum negative enhancement time and enhancement disappearance time with our contrast are earlier than those of previously reported contrasts. The time intervals between the MRI scans in our mice study were

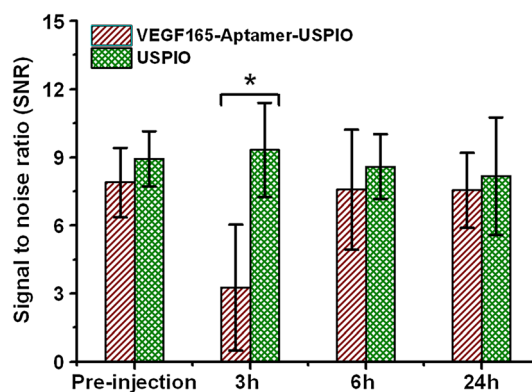


**Figure 6.** Signal to noise ratio in the tumor with VEGF165-aptamer-USPIO probe and USPIO nanoparticles administered at a dosage of 9.08 nmol/kg body weight in nude mice ( $*p < 0.05$ ).

longer than optimal. A more refined time-enhancement curve can be built with shorter scan intervals, which will be completed and improved upon in future studies.

To further confirm the presence of VEGF165-aptamer-USPIO probe in the tumor tissue, the Prussian blue method was carried out on tumor tissue sections of mice sacrificed 3 h after intravenous injection. Obvious Prussian blue-positive stain was observed in the tumor tissue section (Fig. 7B), revealing the presence of the VEGF165-aptamer-USPIO probe in tumor tissue. Moreover, the presence of VEGF165 in tumor stroma of liver cancer xenografts was also confirmed by immunohistochemical staining. As shown in Fig. 7(C), the red arrow points to the blue cell nuclei and the

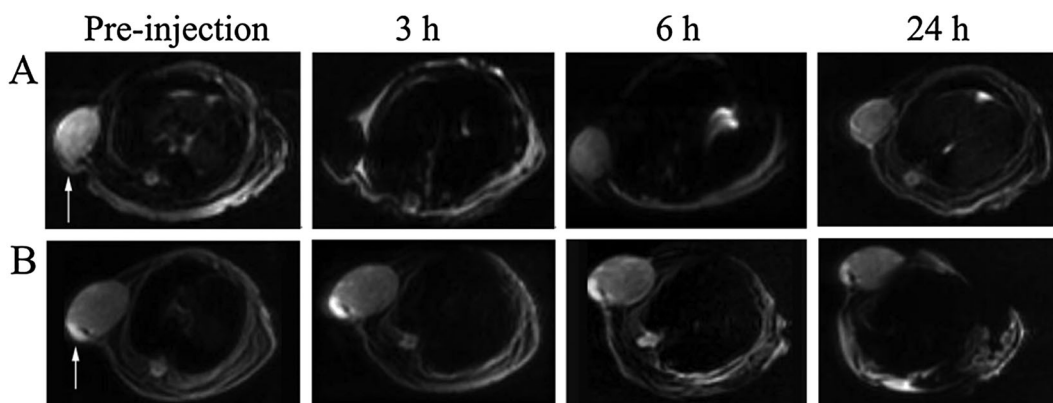


**Figure 5.**  $T_2$ -weighted MRI images of xenograft-bearing nude mice injected with VEGF165-aptamer-USPIO probe (A) and USPIO nanoparticles only (B) from tail vein at a dosage of 9.08 nmol/kg body weight. Arrows point to tumor xenografts.

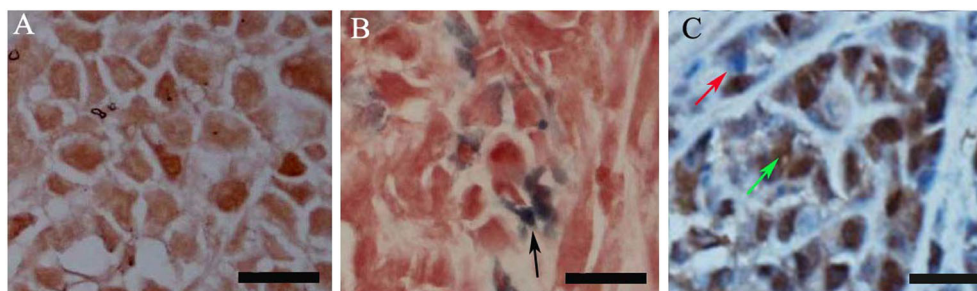


**Figure 7.** Cytochemistry staining images of tumor xenografts in athymic mice with the Prussian blue method, showing Prussian blue-negative (A) staining of USPIO and Prussian blue-positive (B) staining of VEGF165-aptamer-USPIO nanoparticles in the tumor stroma. Immunostaining of VEGF165 in liver tumor xenograft with anti-VEGF165 primary antibody, showing a large quantity of VEGF165 in the tumor stroma (C). Black arrow points to the VEGF165-aptamer-USPIO nanoparticles (B), red arrow shows the nuclei (blue) and green arrow points to the VEGF165 (dark brown) (C). Scale bar = 20  $\mu\text{m}$ .

green arrow points to the dark VEGF165 in tumor cell stroma. The presence of VEGF165 in the tumor stroma was clearly observed after staining with the anti-VEGF165 antibody through 3,3'-diaminobenzidine, which allows the specific binding of the VEGF165-aptamer-USPIO probe in the tumor tissue. All of these results demonstrate that the negative enhancement of the tumor tissue can be attributed to the specific accumulation of the VEGF165-aptamer-USPIO probe in the tumor xenograft through the interaction of aptamer with VEGF165.

### 3. CONCLUSIONS

A MRI molecular probe targeting VEGF165 has been prepared by crosslinking USPIO to the aptamer for VEGF165. The particle size, magnetic property, *in vitro* VEGF165-binding activity and *in vivo*  $T_2$ WI signal enhancement profile suggest that VEGF165-aptamer-USPIO probe is a promising targeted MRI contrast agent, which should be further explored.

## 4. EXPERIMENTAL

### 4.1. Construction of VEGF165-aptamer-USPIO Molecular Probe

Fifty microliters of dextran-coated USPIO (1.5 mg/ml, USPIO concentration, Northwest University, China) was activated by the addition of 200  $\mu\text{l}$  EDC (5 mg/ml, Thermo Fisher Scientific) and 200  $\mu\text{l}$  NHS (5 mg/ml, Thermo Fisher Scientific), and incubated at 37  $^{\circ}\text{C}$  with shaking for 30 min. The reaction mixture was centrifuged at 9600 rpm for 10 min, and the supernatants with unreacted EDC and NHS were discarded. One milligram of VEGF165-aptamer (customer synthesized by Dalian Takara Bioengineering Ltd) was added, the total volume was adjusted to 500  $\mu\text{l}$  using phosphate buffered saline (PBS), and the coupling reaction was allowed to proceed for 3 h. Unreacted VEGF165-aptamer was removed using centrifugation (9600 rpm, 10 min), and the supernatant was discarded. The product was stored at 4  $^{\circ}\text{C}$  until use (21).

### 4.2. ELISA *in vitro* Binding Assay

In each centrifuge tube, 0.25 ml VEGF165-aptamer-USPIO probe (1.0 mg/ml, USPIO concentration) was incubated with 0.125  $\mu\text{g}$  VEGF165 (ProSpec-Tany TechnoGene Ltd) in 0.25 ml PBS (0.1 M, pH 7.4) for 1 h at 37  $^{\circ}\text{C}$  with shaking. VEGF165 was replaced by the same amount of VEGF121 in the negative control group, and VEGF165-aptamer-USPIO was replaced by the same amount of USPIO in the blank group. The solution was centrifuged at

9600 rpm for 10 min, and the pellet was incubated for 30 min with 50  $\mu\text{l}$  anti-VEGF165 monoclonal antibody (1:500 dilution, Millipore). The liquid was removed by centrifugation. The pellet was rinsed with PBS, and incubated for 30 min with 50  $\mu\text{l}$  horseradish peroxidase labeled anti-rabbit IgG sheep antibody (1:1000 dilution, Millipore). Two hundred microliters of chromogenic solution A and B, hydrogen peroxide and tetramethylbenzidine solution (InTec Ltd) were added and incubated for 20 min before the reactions were stopped with the addition of 100  $\mu\text{l}$  stop buffer. The reaction mixtures were centrifuged, 50  $\mu\text{l}$  supernatant was transferred from each tube to a 96-well ELISA plate, and the absorption at 450 nm was obtained using a microplate reader (model MK3, Thermo Scientific).

### 4.3. CCK-8 Cell Proliferation Assay

Human umbilical vein endothelial cells (School of Medicine, Shanghai Jiaotong University) were cultured in 96-well plates with 0.1 ml of RPMI-1640 medium for 18 h (Costar-Corning). To each well were added 50  $\mu\text{l}$  of VEGF165 (40 ng/ml) and various volumes (0, 75, 37.5, 18.75 and 0  $\mu\text{l}$ ) of 1.5 mg/ml VEGF165-aptamer-USPIO probe aqueous solution (Table 2). The blank control wells contained neither VEGF165 nor VEGF165-aptamer-USPIO probe (group 1). Only 50  $\mu\text{l}$  of VEGF165 (40 ng/ml) was added to the positive control (group 5). The cells were cultured at 37  $^{\circ}\text{C}$  for an additional 48 h. A cell counting kit-8 (CCK-8, Beyotime Institute of Technology Ltd) assay was performed according to the protocol from the manufacturer. Twenty microliters of CCK-8 reagent was added to each well, and the solutions were incubated for 4 h before the absorption at 450 nm was determined using a microplate reader.

### 4.4. MRI $T_2$ WI Enhancement Test in Liver Cancer Xenograft Mice

Fifteen nude mice bearing human liver carcinoma cells BEL-7402 subaxillary xenograft (male mice, 25–30 g, tumor diameter about 1.0 cm, purchased from Shanghai Slac Laboratory Animals Ltd) were randomly divided into experimental and control groups. After the animals were anesthetized with pentobarbital (0.05 mg/g, i.p.), seven mice in the experimental group were each given 0.3 ml VEGF165-aptamer-USPIO (10 mg/ml,  $7.57 \times 10^{-10}$  mol/ml) through the tail vein, while the other eight mice in the control group received the same amount of USPIO through the same route. The scans were completed using a 3.0 T MRI (GE, Pittsburgh, PA USA) with a dedicated mouse MRI coil (Shanghai Chenguang Medical Technologies Ltd). Four scans were performed on each animal. The first scan was performed before contrast administration; the other scans were performed 3, 6 and 24 h

post-injection. All scans were conducted under the following conditions: axial fast spin echo  $T_2$ -weighted imaging; repetition time, 4000 ms; echo time, 102 ms; number of excitations, 4; matrix,  $192 \times 192$ ; field of view,  $8 \times 8$  cm; slice thickness, 0.8 mm; slice interval, 0.1. The signal intensity was obtained by averaging the three measurements for three regions of interest within the same slice at various timeframes. The diameter of each region of interest is roughly 2.0 mm. This animal study was approved by the independent Ethics Committee of Hainan Medical College Hospital, and all study animals received humane care throughout this study.

#### 4.5. Tumor VEGF165 Immunohistology

Immunohistological staining of 7402 liver cancer mice xenograft (Shanghai Slac Laboratory Animals Ltd) was performed as reported (23). Briefly, the tumor tissue of mice ( $n=3$ ) injected with VEGF165-aptamer-USPIO was fixed in 4% formaldehyde, dehydrated in graded alcohol and xylene, and embedded in paraffin. Tumor tissue of mice ( $n=3$ ) injected with USPIO was used as a control. The tissue block was sectioned at  $5 \mu\text{m}$  thickness and mounted onto slides, which were kept at  $60^\circ\text{C}$  overnight. The sections were sequentially immersed in xylene twice each for 5 min and in grade alcohol. The samples were rinsed with water and 0.1 M PBS, and then immersed in methanol with 1% hydrogen peroxide at room temperature for 10 min, before a final water rinse. The sections were treated with antigen retrieval agent, rinsed with water, and blocked with non-immune horse serum. The samples were incubated with anti-VEGF165 antibody (Sigma) at  $4^\circ\text{C}$  overnight, followed by a wash with 0.1 M PBS. The samples were then incubated with biotinylated secondary antibody (Sigma) for 20 min at  $37^\circ\text{C}$ , followed by a PBS rinse. The sections were incubated with streptavidin-horseradish peroxidase at  $37^\circ\text{C}$  for 20 min, and washed with PBS. The color was developed with chromagen 3,3'-diaminobenzidine, and thoroughly washed with water. The sections were finally counterstained with hematoxylin.

For Prussian blue staining, tumor tissue sections embedded in paraffin were immersed in xylene and washed with ethanol-water, incubated for 30 min with 2% potassium ferrocyanide in 6% hydrochloric acid, washed and counterstained with nuclear fast red.

#### 4.6. Statistical Analysis

Statistical analyses were conducted using SPSS 11.5 and Excel 2003. Quantitative data from the experimental and control groups were compared using the least significant difference  $t$ -test. Differences with  $p < 0.05$  were considered to be statistically significant.

### Acknowledgments

This research was supported by National Nature Science Foundation of China (grant no. 30760059 and 81160177), the Hainan Province Key Science and Technology Project Fund (grant no. 070209) and Innovation Introduction Integrated Special Science Cooperation Project of Hainan Province (KJHZ2013-05).

### REFERENCES

- Hak S, Reitan NK, Haraldseth O, *et al.* Intravital microscopy in window chambers: a unique tool to study tumor angiogenesis and delivery of nanoparticles. *Angiogenesis* 2010; 13(2): 113–130; doi: 10.1007/s10456-010-9176-y
- Hicklin DJ, Ellis LM. Role of the vascular endothelial growth factor pathway in tumor growth and angiogenesis. *J Clin Oncol* 2005; 23(5): 1011–1027; doi: 10.1200/JCO.2005.06.081
- Sauter ER, Nesbit M, Watson JC, *et al.* Vascular endothelial growth factor is a marker of tumor invasion and metastasis in squamous cell carcinomas of the head and neck. *Clin Cancer Res* 1999; 5(4): 775–782.
- Jayson GC, Zweit J, Jackson A, *et al.* Molecular imaging and biological evaluation of HuMV833 anti-VEGF antibody: implications for trial design of antiangiogenic antibodies. *J Natl Cancer Inst* 2002; 94(19): 1484–1493; doi: 10.1093/jnci/94.19.1484
- Nagengast WB, de Korte MA, Oude Munnink TH, *et al.*  $^{89}\text{Zr}$ -bevacizumab PET of early antiangiogenic tumor response to treatment with HSP90 inhibitor NVP-AUY922. *J Nucl Med* 2010; 51(5): 761–767; doi: 10.2967/jnumed.109.071043
- Anderson CR, Rychak JJ, Backer M, *et al.* scVEGF microbubble ultrasound contrast agents: a novel probe for ultrasound molecular imaging of tumor angiogenesis. *Invest Radiol* 2010; 45(10): 579–585; doi: 10.1097/RLI.0b013e3181efd581
- Liu Y, Chen Z, Liu C, Yu D, *et al.* Gadolinium-loaded polymeric nanoparticles modified with Anti-VEGF as multifunctional MRI contrast agents for the diagnosis of liver cancer. *Biomaterials* 2011; 32(22): 5167–5176; doi: 10.1016/j.biomaterials.2011.03.077
- Cho EJ, Lee JW, Ellington AD. Applications of aptamers as sensors. *Annu Rev Anal Chem* 2009; 2: 241–264; doi: 10.1146/annurev.anchem.1.031207.112851
- Soontornworajit B, Wang Y. Nucleic acid aptamers for clinical diagnosis: cell detection and molecular imaging. *Anal Bioanal Chem* 2011; 399(4): 1591–1599; doi: 10.1007/s00216-010-4559-x
- Cerchia L, de Franciscis V. Targeting cancer cells with nucleic acid aptamers. *Trends Biotechnol* 2010; 28(10): 517–525; doi: 10.1016/j.tibtech.2010.07.005
- Lee JH, Canny MD, Erkenez AD, *et al.* A therapeutic aptamer inhibits angiogenesis by specifically targeting the heparin binding domain of VEGF165. *Proc Natl Acad Sci U S A* 2005; 102(52): 18902–18907; doi: 10.1073/pnas.0509069102
- Liu Z, Wang F. Dual-targeted molecular probes for cancer imaging. *Curr Pharm Biotechnol* 2010; 11(6): 610–619. PII:BSP/CPB/E-Pub/0084-11-6
- Chen K, Chen X. Design and development of molecular imaging probes. *Curr Top Med Chem* 2010; 10(12): 1227–1236; PII: BSP/CTMC/E-Pub/-0071-10-11
- Lee S, Xie J, Chen X. Activatable molecular probes for cancer imaging. *Curr Top Med Chem* 2010; 10(11): 1135–1144; PII:BSP/CTMC/E-Pub/-0065-10-11
- John R, Boppert SA. Magnetomotive molecular nanoprobe. *Curr Med Chem* 2011; 18(14): 2103–2114; PII:BSP/CMC/E-Pub/2011/148
- Bogdanov A Jr, Mazzanti ML. Molecular magnetic resonance contrast agents for the detection of cancer: past and present. *Semin Oncol* 2011; 38(1): 42–54; doi: 10.1016/j.biomaterials.2010.10.034
- Ko HY, Choi KJ, Lee CH, *et al.* A multimodal nanoparticle-based cancer imaging probe simultaneously targeting nucleolin, integrin  $\alpha v \beta 3$  and tenascin-C proteins. *Biomaterials* 2011; 32(4): 1130–1138; doi: 10.1016/j.biomaterials.2010.10.034
- Li S, He H, Cui W, *et al.* Detection of A $\beta$  plaques by a novel specific MRI probe precursor CR-BSA-(Gd-DTPA) $_n$  in APP/PS1 transgenic mice. *Anat Rec* 2010; 293(12): 2136–2143; doi: 10.1002/ar.21209
- Wang AZ, Bagalkot V, Vasiliiou CC, *et al.* Superparamagnetic iron oxide nanoparticle-aptamer bioconjugates for combined prostate cancer imaging and therapy. *Chem Med Chem* 2008; 3(9): 1311–1315; doi: 10.1002/cmcd.200800091
- Liu Z, Zhao Y, Li J, *et al.* The venom of the spider *Macrothele raveni* induces apoptosis in the myelogenous leukemia K562 cell line. *Leuk Res* 2012; 36(8): 1063–1066.
- Hsieh WJ, Liang CJ, Chieh JJ *et al.* In vivo tumor targeting and imaging with anti-vascular endothelial growth factor antibody-conjugated dextran-coated iron oxide nanoparticles. *Int J Nanomed* 2012; 7: 2833–2842; doi: 10.2147/IJN.S32154
- Leung K. Ovarian cancer antigen 183B2 monoclonal antibody conjugated to ultrasmall superparamagnetic iron oxide nanoparticles. *Molecular Imaging and Contrast Agent Database*. National Center for Biotechnology Information: Bethesda MD, 2004–2011 (updated 14 April 2011). Book accession: NBK53963.
- Spanholtz TA, Theodorou P, Holzbach T, *et al.* Vascular endothelial growth factor (VEGF165) plus basic fibroblast growth factor (bFGF) producing cells induce a mature and stable vascular network – a future therapy for chemically challenged tissue. *J Surg Res* 2011; 171(1): 329–338; doi: 10.1016/j.jss.2010.03.033